Investigation of Collisional Quenching of CCl_2 ($\tilde{A}^1B_1$) in Different Vibrational States

Yide Gao, Yang Chen, Qin Ran, Xingxiao Ma, and Congxiang Chen*

Open Laboratory of Bond Selective Chemistry and Department of Chemical Physics, University of Science and Technology of China, Hefei, Anhui 230026, P. R. China

Received: July 2, 2001; In Final Form: September 4, 2001

CCl_2 free radicals were produced by a pulsed dc discharge of CCl_4 (in Ar). Ground eletronic state CCl_2 ($\tilde{X}$) radicals were electronically excited to $\tilde{A}\ ^1B_1$ (0,3,0), (0,4,0), (1,3,0), (0,6,0), (1,4,0), and (2,2,0) vibronic states by a Nd:YAG laser pumped dye laser at 550.56, 541.52, 532.25, 524.31, 523.82, and 523.37 nm, respectively. Experimental quenching data of excited $CCl_2(\tilde{A}^1B_1$ and $\tilde{a}^3B_1)$ by CH_3OH, C_2H_5OH, n-C_3H_7OH, n-C_4H_9OH, CH_2Br_2, CH_3COCH_3, $CH_3COC_2H_5$, $NH(CH_3)_2$, $NH(C_2H_5)_2$, $N(C_2H_5)_3$, and n-C_6H_{14} molecules were obtained by observing the time-resolved total laser induced fluorescence(LIF) signal of the excited CCl_2 radical, which showed a superposition of two exponential components under the presence of quencher. The quenching rate constants of the $\tilde{A}(^1B_1)$ and $\tilde{a}(^3B_1)$ states of CCl_2, k_A and k_a , were derived by analyzing the experimental data according to a proposed three-level-model to deal with the CCl_2 ($\tilde{X}^1A_1$, $\tilde{A}^1B_1$, $\tilde{a}^3B_1$) system. It is found that the total collisional quenching rate constants of CCl_2 $\tilde{A}^1B_1$ are independent of its vibronic states for a given collisional partner.

Introduction

Although Geuther[1] suggested that dichlorocarbene is involved in the alkaline hydrolysis of chloroform in 1862, Hine[2] substantiated it experimentally just in 1950. From then on, much effort has gone into the study of the role played by CCl_2 as an intermediate of some organic chemical reactions.[3−7] Thus direct spectroscopic observation of this species would be of considerable interest to both chemists and physicists.[8−25] But only a few studies on kinetics of CCl_2 radicals have been reported. In 1977 Huie et al.[14] produced CCl_2 radicals by passing $CF_2{=}CCl_2$ through a microwave discharge of O_2. The dominant initial step is

$$O(^3P) + CF_2{=}CCl_2 \rightarrow CF_2O + CCl_2$$

The radiative lifetimes and quenching rate constants by O_2 were measured by ($\tilde{A}-\tilde{X}$) laser induced fluorescence (LIF) spectroscopy using laser excitation at 515, 484, 445, and 437 nm wavelengths, respectively. In 1980, Tiee et al.[17] measured the rate constants for the reaction of the CCl_2 radical with NO, O_2, F_2, CO, C_3H_8, C_2H_4, and Ar. The CCl_2 radical was generated by photolysis of a halogenated hydrocarbon and probed in a time-resolved manner via LIF using a tunable dye laser. In 1986, Ibuki et al.[20] measured the emission spectrum of the excited CCl_2, which was generated by the direct photodecomposition of CCl_4 and $CBrCl_3$ molecules using H Lyman-α, Ar I resonance lines and synchrotron radiation. They observed the fluorescence decay curve and found that the decay curve is a superposition of two lifetime components. In addition, the quenching rate constants of $CCl_2(\tilde{A}^1B_1)$ by CCl_4 and $CBrCl_3$ were measured. In 1989, Ibuki et al.[21] generated the CCl_2 radical again by the photodecomposition of C_2Cl_6 using synchrotron radiation and obtained kinetic results similar to those in ref 20. In 1996, Wagner[26] produced $CCl_2(\tilde{X})$ radicals by the chemical reaction and measured the reaction rate constant between the ground-state CCl_2 and Cl_2. In 2000, Merelas et al.[27] measured the rate constants for the collisional removal of CCl_2 at room temperature, which was generated by IRMPD of $CF_2{=}CCl_2$, in its $\tilde{X}^1A_1(0,0,0)$ state and $\tilde{A}^1B_1(0,7,0)$ state by several simple alkenes, $CF_2{=}CCl_2$, He, Ar, etc. Recently we have reported[28−31] the kinetic results of the collisional quenching of CCl_2 $\tilde{A}^1B_1$ (0,4,0) by alcohols, substituted methanes, alkanes, and ketones.

It is interesting to assess the collision complex model and, further, to get some important information about the complex formation mechanism between $CCl_2(\tilde{A})$ and the partner, such as the reaction barrier and the role played by the attractive forces between the collisional partners. In this work, we are especially interested in the kinetic behavior for the different vibrational states of electronically excited CCl_2 $\tilde{A}^1B_1$. CCl_2 free radicals were produced by a pulsed dc discharge of CCl_4 (in Ar). Ground electronic state CCl_2 ($\tilde{X}$) radical was electronically excited to the $\tilde{A}^1B_1$ (0,3,0), (0,4,0), (1,3,0), (0,6,0), (1,4,0), and (2,2,0) vibronic states by a Nd:YAG laser pumped dye laser at 550.56, 541.52, 532.25, 524.31, 523.82, and 523.37 nm, respectively. Experimental quenching data of excited $CCl_2(\tilde{A}^1B_1$ and $\tilde{a}^3B_1)$ in the presence of CH_3OH, C_2H_5OH, n-C_3H_7OH, n-C_4H_9OH, CH_2Br_2, CH_3COCH_3, $CH_3COC_2H_5$, $NH(CH_3)_2$, $NH(C_2H_5)_2$, $N(C_2H_5)_3$, and n-C_6H_{14} molecules, which have strong polarities and polarizabilities although with different values, were obtained by observing the time-resolved total laser induced fluorescence (LIF) signal of the excited CCl_2 radical. The signal profile shows a superposition of two exponential components under the presence of quencher. The quenching rate constants of $\tilde{A}(^1B_1)$ and $\tilde{a}(^3B_1)$ states of CCl_2, k_A and k_a, were derived by analyzing the experimental data according to a proposed three-level model to deal with the CCl_2 ($\tilde{X}^1A_1$, $\tilde{A}^1B_1$, $\tilde{a}\ ^3B_1$) system.

Experimental Section

The dc discharge-LIF kinetic experimental setup, described in detail previously,[28−31] involves a pulsed dc discharge, gas handling system, reactor, laser source, signal detection, data

---

* To whom correspondence should be addressed. E-mail address: cxchen@ustc.edu.cn. Fax: 86-551-3607084.

10.1021/jp0124995 CCC: $20.00

processing system, and time sequence system. The supersonic jet apparatus is basically similar to that described in detail previously,[25] where the LIF signal is observed under collisionless conditions in order to compare the LIF signal profiles under cell and supersonic jet conditions.

The dc discharge system includes a high-voltage power supply and a discharge cavity. Its core part is a polytetrafluoroethylene discharge head with 1 mm diameter gas pathway, which is screwed on a movable stainless steel tube and located on the upstream of the reaction vessel. A pair of tungsten pins with a space of 0.5 mm was put into the head perpendicularly to the gas pathway. The pins were fixed onto the discharge head by two screw nails acting as both power terminal and rivet. The power source consists of a silicon-controlled rectifier and a pulsed high-voltage transformer with a turn ratio of 1:100 and the primary voltage is adjustable. The pulsed dc discharge is initiated between the pair of tungsten needles. The discharge cavity is set at right angle to the laser beam. The distance between the discharge and the laser beam was adjusted by moving the stainless steel tube, and was 30 mm in this work.

The experiments were performed in a stainless steel reactor by using steady-flow technique. The reactor, gas handling system and control of flow velocity were described in detail previously.[28−31] The precursor molecule CCl_4 and the quenching molecules were diluted in a large excess of Ar and stored in 10 l reservoirs prior to experiments. Three gas mixtures were slowly flowing into the reaction vessel: f_1, the flow of about 1% CCl_4 in Ar; f_2, the flow of a quenching molecule mixed with Ar; and f_3, the flow of pure Ar. In the reaction vessel, the total pressure P_{total} was about 200 Pa and the partial pressure of CCl_4, P_{CCl_4}, was about 0.5 Pa. In our experiments, P_{total} and P_{CCl_4} were kept constant. The gases in the vessel were renewed in 0.1 s in order to prevent accumulation of the discharge-produced species and reaction products. The ground state CCl_2 radical was electronically excited to the $\tilde{A}\ ^1B_1(n_1,\ n_2,\ 0)$ state by a dye laser (Lumonics, HD500) pumped by a Nd:YAG laser (Spectra Physics, GCR-170, repetition rate of 10 Hz). The spot diameter of the dye laser beam was about 4 mm. The fluorescence signal was transmitted through a cutoff filter with transmitting wavelengths longer than 565 nm and was monitored by a photomultiplier (PMT) (GDB56, Beijing). The PMT output was detected by a digital storage oscilloscope (TDS380, Tektronix) or recorded by a transient digitizer and then averaged by a computer data acquisition system. In our experiment, the signal was averaged over 1000 laser shots. To avoid the mutual disturbing between the laser and discharge system, two photoelectronic isolators were connected between the multichannel delay generator and laser, and between the multichannel delay generator and discharge system, respectively. The triggering of the discharge, YAG laser, and signal acquisition system were controlled by the multichannel pulse generator sequentially.

In our supersonic jet apparatus used in this work, the sample gas seeded in Ar at stagnation pressure of 5 atm flowed through a pulsed nozzle (General valve) of 0.5 mm orifice diameter into an expansion chamber at a repetition rate of 10 Hz. CCl_2 radicals were produced by discharge. The light source and signal detector were the same as aforementioned. The operations of the pulsed nozzle, discharge, YAG laser, and signal acquisition were controlled by the multichannel pulse generator sequentially.

Ar (99.999%, Nanjing) was taken from cylinders without further purification. CCl_4, CH_3OH, C_2H_5OH, n-C_3H_7OH, n-C_4H_9OH, CH_2Br_2, CH_3COCH_3, $CH_3COC_2H_5$, $NH(CH_3)_2$, $NH(C_2H_5)_2$, $N(C_2H_5)_3$, and n-C_6H_{14}, of analytical reagent grade, were carefully degassed, further purified by freeze−pump−thaw cycles in a vacuum system, vaporized into reservoirs, and mixed with bath gas Ar before use.

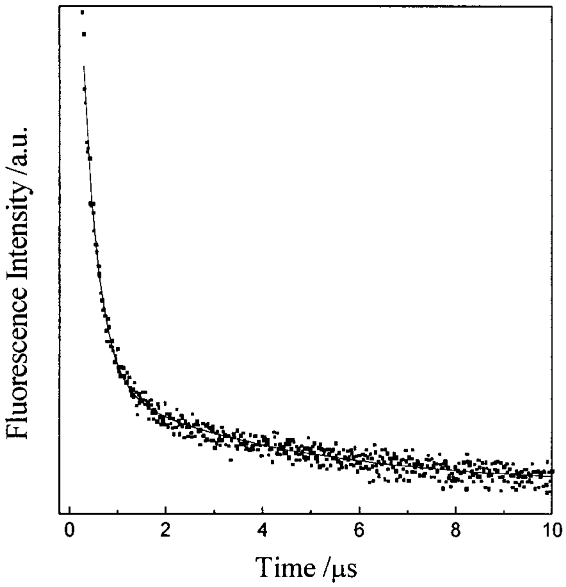

Figure 1. A typical LIF decay profile of the electronically excited CCl_2 quenched by CH_3OH: dots are the experimental data and solid line is the fitting result. The excitation wavelength is 550.56 nm.

Results and Discussion

A. Identification of CCl_2 Radical. To identify that the CCl_2 radicals were the only species detected in the excitation wavelength region in this work, we observed laser-induced fluorescence excitation spectrum of gas-phase CCl_2 produced by dc discharge and cooled in a supersonic free jet over the 440−580 nm region. The result is in good agreement with the low-resolution jet fluorescence excitation spectrum of CCl_2 in the 530−555 nm region for both the peak-outline and peak-positions.[24] Meanwhile, we have determined a higher resolution jet cooled LIF spectrum, which is identical to a reported progression of bands of CCl_2 radical in the 497−534 nm region with k-structure resolved.[23, 25.] It means that we have reliably detected CCl_2 radicals.

B. Description of the Kinetic Model. A typical time-resolved fluorescence signal of the $CCl_2(\tilde{A}\ ^1B_1)$ radical is shown in Figure 1, in which the quenching process by CH_3OH takes place under the conditions of total pressure of 200 Pa.

The decay profile was fitted to

$$y = A_1 \exp(-k_1 t) + A_2 \exp(-k_2 t) \tag{1}$$

It can be seen that the decay curve may be satisfactorily analyzed as a superposition of two lifetime components. In contrast, we have measured the time-resolved LIF signal in supersonic free jet conditions, which is shown in Figure 2. It can be considered that there is no collision between molecules under the supersonic jet conditions. In Figure 2 it can be seen that it is a monoexponential decay curve corresponding to the decay of the $\tilde{A}$ state. This indicates that the superposition of two lifetime components is caused by collisions.

Nguyen et al.[32] had calculated the energy levels of the CCl_2 radical and found an $\tilde{a}^3B_1$ state lying between $\tilde{A}^1B_1$ and $\tilde{X}^1A_1$, which is 0.95 eV higher than the ground state. Ibuki[20] speculated that the collision-induced intersystem crossing between the $^1B_1$ and $^3B_1$ states plays an important role in giving rise to the nonexponential behavior. That is, the vibrationally hot CCl_2 $(\tilde{A}^1B_1)$ radicals produced in the primary excitation process are

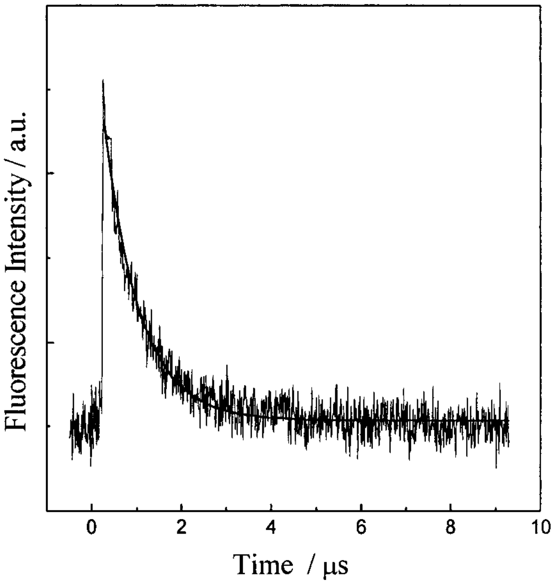

Figure 2. Time-resolved LIF signal of jet-cooled $CCl_2(^1B_1)$. Excitation wavelength is 550.56 nm.

converted to high vibrationally excited CCl_2 in the $^3B_1$ state due to the bimolecular collisions. Since the phosphorescence lifetime of the CCl_2 ($\tilde{a}^3B_1 \rightarrow \tilde{X}^1A_1$) transition is expected to be very long, the hot CCl_2 ($\tilde{a}^3B_1$) radical would be again quenched to the lower vibrational levels of the $\tilde{A}^1B_1$ state.

Thayer and Yardley [33] found that collisions could induce intramolecular excitation transfer. They observed that electronically excited propynal molecules were very efficiently quenched by molecules with large permanent dipole moments, although electronic transfer to the collision partners is not energetically possible in these experiments. They suggested that the permanent dipole moment of the quencher can induce an energy-conserving transition within propynal if the two states involved are connected by a dipole matrix element. These authors have also pointed out that, even for collision partners with no net dipole moment, electrostatic interactions can in second order induce similar electronic transfer processes. Thus, we proposed following collisional kinetic mechanism for the quenching of electronically excited CCl_2 radicals.[28−31]

$$CCl_2(\tilde{X}^1A_1) + h\nu \rightarrow CCl_2(\tilde{A}^1B_1) \quad (2)$$

$$CCl_2(\tilde{A}^1B_1) + Q(M) \xrightarrow{k_{q1}(k_{m1})} CCl_2(\tilde{X}^1A_1) + Q\ (M) \text{ or other products} \quad (3)$$

$$CCl_2(\tilde{A}^1B_1) + Q(M) \xrightarrow{\xi_{q1}(\xi_{m1})} CCl_2(\tilde{a}^3B_1) + Q(M) \quad (4)$$

$$CCl_2(\tilde{a}^3B_1) + Q(M) \xrightarrow{\xi_{q2}(\xi_{m2})} CCl_2(\tilde{A}^1B_1) + Q(M) \quad (4')$$

$$CCl_2(\tilde{a}^3B_1) + Q(M) \xrightarrow{k_{q2}(k_{m2})} CCl_2(\tilde{X}^1A_1) + Q\ (M) \text{ or other products} \quad (5)$$

$$CCl_2(\tilde{A}^1B_1) \xrightarrow{k_f} CCl_2(\tilde{X}^1A_1) + h\nu_f \quad (6)$$

where Q is the quencher. M denotes other molecules (including CCl_4, Ar, and the discharge-produced species, etc.). The concentrations of M were kept constant in our experiment.

Since what we shall discuss afterward is a fast pump process (the pulse width of dye laser is 5 ns) and laser intensity is not too high (3−5 mJ /pulse), we assumed that the pump and dump (laser stimulated emission deexcitation) would not influence the description of the kinetic behavior after the laser irradiation.[34] Immediately, after the laser pulse, it is assumed that the partial densities of CCl_2 ($\tilde{A}$) and ($\tilde{a}$) states are N_A^0 and $N_a^0 = 0$, respectively. k_f represents the Einstein spontaneous emission coefficient from $\tilde{A}$ to $\tilde{X}$. k_{q1} represents the rate constant of chemical reaction of $\tilde{A}$ state and transition of $\tilde{A}^1B_1 \rightarrow \tilde{X}^1A_1$ caused by collision with Q. k_{q2} represents the rate constant of chemical reaction and physical quenching of $\tilde{a}^3B_1$. N_q and N_m are the concentrations of quencher and M, respectively. k_{mi} ($i = 1$ and 2) represents the collisional removal rate constant by M molecules. ξ_i and ξ_{mi} ($i = 1$ and 2) represent the transition rate constants between the $\tilde{A}$ and $\tilde{a}$ states due to the collisions with quencher and M.

The kinetic equations of N_A and N_a can be expressed as

$$\frac{dN_A}{dt} = -k_f N_A - k_{q1} N_q N_A - \xi_1 N_q N_A - k_{m1} N_m N_A - \xi_{m1} N_m N_A + \xi_2 N_q N_a + \xi_{m2} N_m N_a = -AN_A + BN_a \quad (7)$$

where

$$A = k_f + k_{m1}N_m + \xi_{m1}N_m + k_{q1}N_q + \xi_1 N_q \quad (8)$$

and

$$B = \xi_2 N_q + \xi_{m2} N_m \quad (9)$$

and

$$\frac{dN_a}{dt} = \xi_1 N_q N_A + \xi_{m1} N_m N_A - \xi_2 N_q N_a - \xi_{m2} N_m N_a - k_{q2} N_q N_a - k_{m2} N_m N_a = CN_A - DN_a \quad (10)$$

where

$$C = \xi_1 N_q + \xi_{m1} N_m \quad (11)$$

and

$$D = \xi_{m2} N_m + k_{m2} N_m + k_{q2} N_q + \xi_2 N_q \quad (12)$$

Thus, we can arrive at

$$N_A = \frac{1}{\beta - \alpha}\{[(\beta - A)N_A^0 + BNN_a^0]\, e^{-\alpha t} + [(A - \alpha)\, NN_A^0 - BNN_a^0]\, e^{-\beta t}\} \quad (13)$$

and

$$N_a = \frac{1}{\beta - \alpha}\{[CN_A^0 + (A - \alpha)N_a^0]\, e^{-\alpha t} - [CN_A^0 - (\beta - A)N_a^0]\, e^{-\beta t}\} \quad (14)$$

where

$$\alpha + \beta = A + D, \quad \alpha\beta = AD - BC \quad (15)$$

Noting $N_a^0 = 0$, thus

$$N_A = \frac{1}{\beta - \alpha}\{(\beta - A)N_A^0\, e^{-\alpha t} + (A - \alpha)N_A^0\, e^{-\beta t}\} \quad (16)$$

$$N_a = \frac{1}{\beta - \alpha}(CN_A^0\, e^{-\alpha t} - CN_A^0\, e^{-\beta t}) \quad (17)$$

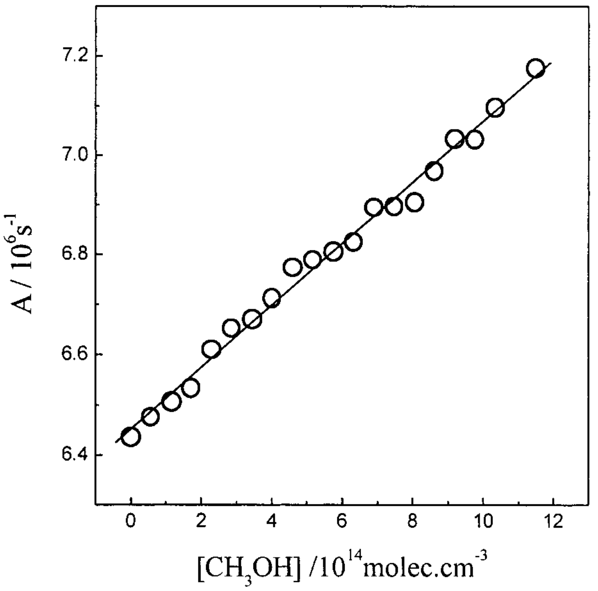

Figure 3. Plot of *A* as a function of concentration of CH_3OH.

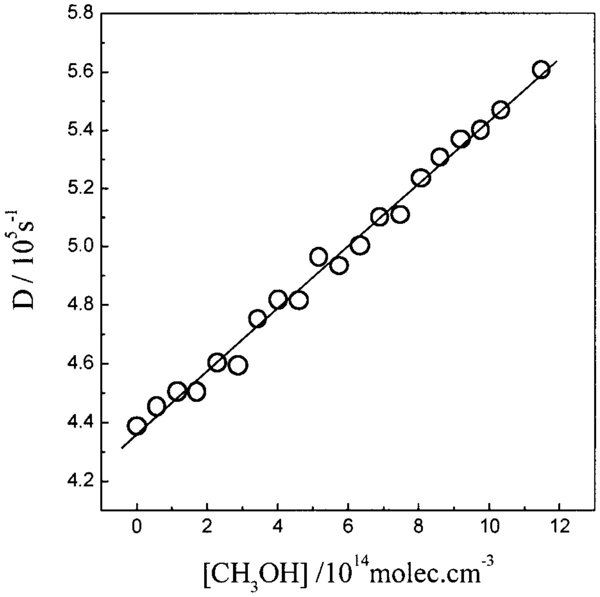

Figure 4. Plot of *D* as a function of concentration of CH_3OH.

Since the fluorescence emission of excited CCl_2 radicals is from Ã state, the detected fluorescence signal intensity is proportional to N_A, i.e.

$$I = \kappa\, k_f\, N_A = \frac{\kappa}{\beta - \alpha} N_A^0\, k_f[(\beta - A)\, e^{-\alpha t} + (A - \alpha)\, e^{-\beta t}] \tag{18}$$

where, κ is the instrument coefficient.

Comparing eq 1 with eq 18,

$$\alpha = k_1, \quad \beta = k_2 \tag{19}$$

$$A_1 = \frac{k}{\beta - \alpha} N_A^0\, k_f\, (\beta - A), \quad A_2 = \frac{\kappa}{\beta - \alpha} N_A^0\, k_f\, (A - \alpha) \tag{20}$$

Thus

$$A_1/A_2 = (\beta - A)/(A - \alpha) \tag{21}$$

$$A = (A_1\alpha + A_2\beta)/(A_1 + A_2) \tag{22}$$

$$D = \alpha + \beta - A \tag{23}$$

C. Determined Results. Before analyzing the time-resolved signal to derive the fluorescence decay rate constant, a small background that resulted from the scattered laser irradiation in the reactor without discharge was subtracted from the gross signal to get a net value. The net time-resolved fluorescence signal of excited CCl_2 radical quenched by CH_3OH at 550.56 nm of excitation wavelength and its fitting to two exponential component decay are illustrated in Figure 1, and the values of A_1, A_2, k_1, and k_2 can be obtained. *A* and *D* can be calculated by eqs 22 and 23. The plots of *A* and *D* vs [CH_3OH] based on eqs 8 and 12 are illustrated in Figures 3 and 4. The slopes of the straight lines are the rate constants $k_A = k_{q1} + \xi_1$ and $k_a = k_{q2} + \xi_2$ of CCl_2(Ã) (0,3,0) and $CCl_2(\tilde{a}^3B_1)$ states quenched by CH_3OH, respectively. It should be indicated that the experiment yielded only two sums of these, k_A (for Ã → X̃, Ã → ã and reaction of Ã state) and k_a (for ã → X̃, ã → Ã and reaction of ã state). The measured quenching rate constants of the excited CCl_2 radical by CH_3OH, C_2H_5OH, n-C_3H_7OH, n-C_4H_9OH, CH_2Br_2, CH_3COCH_3, $CH_3COC_2H_5$, $NH(CH_3)_2$, $NH(C_2H_5)_2$, $N(C_2H_5)_3$, and n-C_6H_{14} molecules are listed in Table 1. The uncertainties of k_A and k_a are the standard deviations of the least-squares fittings.

To compare the quenching activity of the C−H bond with the C−OH bond, the result of CH_4 is included in Table 1. It can be considered that methanol is formed by substituting an OH group instead of an H atom in methane. From Table 1, we can see that the quenching rate constant of methanol is six times as fast as that of methane. It indicates that the OH group of an alcohol plays an important role in the quenching of CCl_2 radical, because there is an OH group in the alcohol molecule resulting in much stronger polarity than that in the methane.[35] The multipole attractive force between CCl_2 and the alcohol molecule is much stronger than that between CCl_2 and the methane molecule. On the other hand, the bond energy of C−H in alcohol is smaller than that of the corresponding C−H bond in the methane molecule[36] due to the induction of the OH group. It appears that the collisional quenching processes of electronically excited CCl_2 radical by alcohols are very effective. Even the rate constant by n-C_6H_{14} is smaller than that by CH_3OH.

The quenching of electronically excited CCl_2 radical by alcohol is a complicated process, including not only physical quenching but also chemical reaction, although we did not recognize the reaction products. It appears that the rate constants for removal of electronically excited CCl_2 increases steadily with increasing the number of C−H bonds contained in the alcohol molecules. Such quasi-linearity suggests that the C−H bonds in alcohol molecules display essentially similar reactivity.

To investigate the effect of substituted alkyl radicals in amine molecules on the quenching rates of electronically excited CCl_2 radicals, we carried out the measurements of quenching rate constants of $CCl_2(\tilde{A}^1B_1$ and $\tilde{a}^3B_1)$ by $(CH_3)_2NH$, $(C_2H_6)_2NH$, and $(C_2H_6)_3N$ molecules. The quenching rate constants of $CCl_2(\tilde{A}^1B_1$ and $\tilde{a}^3B_1)$ by amine molecules are comparable with each other and significantly faster than those by CH_4.[30] The overall quenching includes chemical and physical quenching processes. For chemical quenching, although the reaction mechanism is complicated and not yet clear, it is probably important that the bond energies of C−H in CH_4 are significantly larger than those of N−H in $(CH_3)_2NH$ and $(C_2H_6)_2NH$ and C−N in amine molecules.[37] Therefore, the activation barriers for the reactions between amine molecules and electronically excited CCl_2

TABLE 1: Rate Constants for Collisional Quenching of $CCl_2(\tilde{A}^1B_1)$ in Different Vibrational States and ($\tilde{a}^3B_1$) by Quenchers (k_A and k_a are in 10^{-10} cm^3/molec·s), $T = 293$ K

quencher	excitation wavelength	vibration state	k_A	k_a	ref
CH_4	516.2	0,7,0	1.10 ± 0.11		27
CH_4	541.52	0,4,0	1.07 ± 0.15	0.43 ± 0.08	30
CH_3OH	550.56	0,3,0	6.17 ± 0.18	1.14 ± 0.10	this work
	541.52	0,4,0	6.08 ± 0.21	1.04 ± 0.11	28
	532.25	1,3,0	6.12 ± 0.15	1.11 ± 0.09	this work
	524.31	0,6,0	6.03 ± 0.13	1.07 ± 0.08	this work
	523.82	1,4,0	5.97 ± 0.12	1.05 ± 0.08	this work
	523.37	2,2,0	5.93 ± 0.14	1.01 ± 0.10	this work
C_2H_5OH	550.56	0,3,0	7.39 ± 0.14	2.11 ± 0.11	this work
	541.52	0,4,0	7.54 ± 0.15	2.12 ± 0.13	28
	532.25	1,3,0	8.12 ± 0.18	2.58 ± 0.12	this work
	524.31	0,6,0	7.47 ± 0.19	2.31 ± 0.14	this work
	523.82	1,4,0	7.56 ± 0.17	2.21 ± 0.13	this work
	523.37	2,2,0	7.36 ± 0.18	2.08 ± 0.12	this work
n-C_3H_7OH	550.56	0,3,0	8.71 ± 0.19	3.15 ± 0.17	this work
	541.52	0,4,0	8.73 ± 0.16	3.01 ± 0.28	28
	532.25	1,3,0	8.63 ± 0.15	3.34 ± 0.17	this work
	524.31	0,6,0	8.81 ± 0.13	2.93 ± 0.11	this work
	523.82	1,4,0	8.62 ± 0.17	2.89 ± 0.13	this work
	523.37	2,2,0	8.77 ± 0.15	2.95 ± 0.14	this work
n-C_4H_9OH	550.56	0,3,0	9.99 ± 0.21	3.75 ± 0.17	this work
	541.52	0,4,0	9.73 ± 0.21	3.62 ± 0.22	28
	532.25	1,3,0	9.86 ± 0.18	3.71 ± 0.17	this work
	524.31	0,6,0	9.81 ± 0.19	3.83 ± 0.16	this work
	523.82	1,4,0	9.71 ± 0.16	3.58 ± 0.17	this work
	523.37	2,2,0	9.78 ± 0.17	3.55 ± 0.13	this work
CH_2Br_2	550.56	0,3,0	11.9 ± 0.21	3.60 ± 0.12	this work
	541.52	0,4,0	11.8 ± 0.27	3.36 ± 0.19	29
	532.25	1,3,0	10.9 ± 0.19	3.01 ± 0.15	this work
CH_3COCH_3	550.56	0,3,0	5.04 ± 0.16	1.78 ± 0.10	this work
	541.52	0,4,0	4.87 ± 0.12	1.83 ± 0.09	31
	532.25	1,3,0	4.95 ± 0.14	1.72 ± 0.11	this work
$C_2H_5COCH_3$	550.56	0,3,0	6.13 ± 0.13	2.34 ± 0.10	this work
	541.52	0,4,0	5.93 ± 0.15	2.23 ± 0.12	31
	532.25	1,3,0	6.04 ± 0.12	2.20 ± 0.11	this work
$NH(CH_3)_2$	550.56	0,3,0	7.88 ± 0.19	2.31 ± 0.13	this work
	541.52	0,4,0	7.69 ± 0.23	2.27 ± 0.12	this work
	532.25	1,3,0	7.71 ± 0.18	2.34 ± 0.11	this work
$NH(C_2H_5)_2$	550.56	0,3,0	7.34 ± 0.15	2.25 ± 0.13	this work
	541.52	0,4,0	7.31 ± 0.19	2.32 ± 0.15	this work
	532.25	1,3,0	7.29 ± 0.17	2.41 ± 011	this work
$N(C_2H_5)_3$	550.56	0,3,0	7.21 ± 0.19	2.22 ± 0.14	this work
	541.52	0,4,0	7.24 ± 0.22	2.11 ± 0.13	this work
	532.25	1,3,0	7.35 ± 0.17	2.18 ± 0.12	this work
n-C_6H_{14}	550.56	0,3,0	4.06 ± 0.10	3.07 ± 0.09	this work
	541.52	0,4,0	3.95 ± 0.05	2.99 ± 0.07	30
	532.25	1,3,0	3.89 ± 0.09	2.98 ± 0.09	this work

radicals would be lower than those between CH_4 and excited CCl_2. On the other hand, for energy transfer processes, because amine molecules are much larger and have many more vibrational modes and therefore much higher state densities, the cross sections of the electronic to vibrational energy transfer between electronically excited CCl_2 radicals and amine molecules would be larger than those between electronically excited CCl_2 radicals and CH_4. For the three amine molecules, within uncertainty, the quenching rate constants are not significantly different from each other.

From Table 1, we can see that the quenching rate constants of alcohol are faster than ketone compounds containing the same number of carbon atoms as in alcohol, indicating that the quenching activity of ketone molecules is less effective than that of alcohol molecules.

TABLE 2: Calculated Complex Formation Cross Sections σ_{cf} of $CCl_2(\tilde{A})$ with Quenchers and Parameters Used in the Calculation (α is in 10^{-24} cm^3 and Q is in 10^{-26} esu·cm^3), $T = 293$ K

quencher	μ^a (D)	α^a	Q^b	I.P.^{a} (eV)	σ_q, $(k_A)^c$ (10^{-2} nm^2)	calc. $\sigma_{cf}{}^d$ (10^{-2} nm^2)
CH_3OH	1.70	3.29	0.50	10.84	117.3	145.3
C_2H_5OH	1.69	5.11	1.65	10.49	164.7	158.6
n-C_3H_7OH	1.68	6.74	2.40	10.10	206.9	167.8
n-C_4H_9OH	1.66	8.88	3.00	10.04	244.4	177.6
CH_3COCH_3	2.88	6.39	3.4	9.69	114.3	198.7
n-C_6H_{14}	0.05	11.9	3.00	10.2	103.1	154.6
CH_2Br_2	1.43	9.32	5.50	9.32	255.0	178.3
$NH(CH_3)_2$	1.03	6.37	4.50	8.24	167.0	152.3
$NH(C_2H_5)_2$	0.92	10.2	4.00	8.01	182.4	164.1
$N(C_2H_5)_3$	0.66	13.1	3.30	7.50	196.3	165.7
CCl_2	0.48^e	6.55^e	0.31^e	7.95^e		

[a] Reference 35, 43. [b] Estimated following ref. 44 and 45. [c] Calculated according to k_A of CCl_2 ($\tilde{A}$) (0,4,0) vibronic state. [d] Calculated using the most favorable orientation method. [e] Reference 27.

By changing the excitation wavelength, the ground electronic state CCl_2 ($\tilde{X}$) radical was electronically excited to different vibronic state of $\tilde{A}^1B_1$. We have obtained the dependence of the collisional quenching result on the vibronic state of CCl_2 ($\tilde{A}^1B_1$). It is found that the total quenching rate constants are independent of the vibronic state within the experimental uncertainties. It is possible that the reaction between the quencher molecules and CCl_2 ($\tilde{A}^1B_1$) undergoes a process without barrier. According to the above analysis, it might be concluded that the quenching processes of the excited CCl_2 ($\tilde{A}^1B_1$) undergoes no barrier reaction and strongly dependes on the polarities of the quencher.

Fairchild et al.[38] proposed a theoretical method to calculate the complex formation cross section based on a collisional complex model,[39−41] which is most likely applicable in this work. They have chosen all the attractive forces to construct the effective potential and compute the cross section for complex formation, σ_{cf}, numerically. According to this theory, σ_{cf} is calculated on the basis of an effective potential $V_{eff}(r)$ between collisional partners using the most favorable orientation method:[38]

$$V_{eff} = Eb^2/r^2 - C_3/r^3 - C_4/r^4 - C_6/r^6 - C_6'/r^6 \qquad (24)$$

or the averaged orientation method:[42]

$$V_{eff} = Eb^2/r^2 - D_6/r^6 - D_8/r^8 - D_6'/r^6 - C_6'/r^6 \qquad (25)$$

Following this method, we calculated σ_{cf} of CCl_2 ($\tilde{A}^1B_1$) with quenching molecules. The parameters used in the calculation, the experimentally measured quenching cross sections, and calculated complex formation cross sections are summarized in Table 2.

The polarizabilities of amines and alcohols are strong, therefore, it is reasonable to adopt the calculation method of the most favorable orientation method. According to ref 38, the quenching cross section is proportional to the theoretical cross section of complex formation, $\sigma_Q = P\sigma_{cf}$, where P is the probability, namely, that quenching will occur during the residence time of the complex. We have no way of knowing P a priori. Generally, it should be different for different quenchers and less than 1. For the collisional partner studied in this work, the values of P are large, particularly for amines and alcohols; the values of P are somewhat more than 1. It indicates that the state mixing of CCl_2 $\tilde{A}$ and $\tilde{X}$, even including $\tilde{a}$ state, and the product formation of chemical reaction are very efficient once the complex is formed. In addition, it means that the attractive forces between the $CCl_2(\tilde{A})$ and the quencher are very strong, and the complex model even underestimates the quenching efficiency of $CCl_2(\tilde{A})$. Therefore, further theoretical and experimental study on the quenching mechanism of electronically excited CCl_2 radical by amines and alcohols is required.

Acknowledgment. This work was supported by the National Natural Science Foundation (29973038 and 10032050), the Important Program of Academia Sinica (LHD970102), and the National Key Basic Research Special Foundation (G1999075304).

References and Notes

(1) Geuther, A. *Ann. Chem. Pharm.* **1862**, *123*, 121.

(2) Hine, J. *J. Am. Chem. Soc.* **1950**, *72*, 2438.

(3) Doering, W. v. E.; Hoffmann, A. K. *J. Am. Chem. Soc*. **1954**, *76*, 6162.

(4) Sherman, R. H.; Bernstein, R. B. *J. Am. Chem. Soc*. **1951**, *73*, 1376.

(5) Closs, G. L.; Coyle, J. J. *J. Am. Chem. Soc*. **1965**, *87*, 4270.

(6) Moss, R. A. *Acc. Chem. Res*. **1989**, *22*, 15.

(7) Moss, R. A. *Acc. Chem. Res*. **1980**, *13*, 58.

(8) Milligan, D. E.; Jacox, M. E. *J. Chem. Phys.* **1967**, *47*, 703.

(9) Andrews, L. *J. Chem. Phys.* **1968**, *48*, 979.

(10) Jacox, M. E.; Milligan, D. E. *J. Chem. Phys.* **1970**, *53*, 2688.

(11) Shirk, J. S. *J. Chem. Phys.* **1971**, *55*, 3608.

(12) Tevault, D. E.; Andrews, L. *J. Mol. Spectrosc*. **1975**, *54*, 110.

(13) Bondybey, V. E. *J. Mol. Spectrosc*. **1977**, *64*, 180.

(14) Huie, R. E.; Long, N. J. T.; Thrush, B. A. *Chem. Phys. Lett.* **1977**, *51*, 197.

(15) Kiefer, R.; Siegel, A.; Schultz, A. *Chem. Phys. Lett.* **1978**, *59*, 298.

(16) Tiee, J. J.; Wampler, F. B.; Rice, W. W. *Chem. Phys. Lett*. **1979**, *65*, 425.

(17) Tiee, J. J.; Wampler, F. B.; Rice, W. W.*Chem. Phys. Lett*. **1980**, *73*, 519.

(18) Clouthier, D. J.; Karolczak, J. *J. Phys. Chem.* **1989**, *93*, 7542.

(19) Predmore, D. A.; Murray, A. M.; Harmony, M. D. *Chem. Phys. Lett*. **1984**, *110*, 173.

(20) Ibuki, T.; Takahashi, N.; Hiraya, A.; Shobatake, K. *J. Chem. Phys*. **1986**, *85*, 5717.

(21) Ibuki, T.; Hiraya, A.; Shobatake, K. *Chem. Phys. Lett.* **1989**, *157*, 521.

(22) Fujitake, M.; Hirota, E. *J. Chem. Phys*. **1989**, *91*, 3426.

(23) Choe, J. I.; Tanner, S. R.; Harmony, M. D. *J. Mol. Spectrosc.* **1989**, *138*, 319.

(24) Clouthier, D. J.; Karolczak, J. *J. Chem. Phys.* **1991**, *94*, 1.

(25) Lu, Q.; Chen, Y.; Wang, D.; Zhang, Y.; Yu, S.; Chen, C.; Koshi, M.; Matsui, H.; Koda, S.; Ma, X. *Chem. Phys. Lett*. **1991**, *178*, 517.

(26) Wagner, M. *Ber.-Max.-Planck-Inst. Stoemungsforsch.* **1996**, *4*, 76−82.

(27) Merelas, I.; Fernández, J. A.; Puyuelo, P.; Sánchez Rayo, M. N.; Husain, D.; Castaño, F. *Chem. Phys.* **2000**, *254*, 77.

(28) Gao, Y.; Chen, Y.; Ma, X.; Chen, C. *Chem. Phys. Lett.* **2001**, *339*, 209.

(29) Gao, Y.; Chen, Y.; Ma, X.; Chen, C. *Chem. Phys.* **2001**, *269*, 389.

(30) Gao, Y.; Pei, L.; Chen, Y.; Chen, C. *J. Chem. Phys.* **2001**, *114*, 10798.

(31) Gao, Y.; Chen, Y.; Dai, J.; Chen, C. *J. Photochem. Photobio. A*, in press.

(32) Nguyen, M. T.; Kerins, M. C.; Hegarty, A. F.; Fitzpatrick, N. J. *Chem. Phys. Lett*. **1985**, *117*, 295.

(33) Thayer, C. A.; Yardley, J. T. *J. Chem. Phys*. **1972**, *57*, 3992.

(34) Ma, X.; Kong, F. *Laser Chemistry*; University of Science and Technology of China Press: Hefei, 1990; p 30.

(35) Weast, R. C. *CRC Handbook of Chemistry and Physics*, 70th ed.; CRC Press: Boca Raton, Florida, 1989/1990; E59, E70, E87.

(36) Wallington, T. J.; Kurylo, M. T. *J. Phys. Chem.* **1987**, *91*, 5050.

(37) Kerr, J. A. *Chem. Rev.* **1966**, *66*, 465.

(38) Fairchild, P. W.; Smith, G. P.; Crosley, D. R. *J. Chem. Phys*. **1983**, *79*, 1795.

(39) Tully, J. C. *J. Chem. Phys*. **1974**, *61*, 61.

(40) Zahr, G. E.; Preston, R. K.; Miller, W. H. *J. Chem. Phys*. **1975**, *62*, 1127.

(41) Holtermann, D. L.; Lee, E. K. C.; Nanes, R. *J. Chem. Phys*. **1982**, *77*, 5327.

(42) Hirschfelder, J. O.; Curtiss, C. F.; Bird, R. B. *Molecular Theory of Gases and Liquids*; Wiley: New York, 1954.

(43) *CRC Handbook of Chemistry and Physics*, 78th ed.; Lide, D. R., Ed.; CRC Press: Boca Raton, Florida, 1997/1998; Chapter 10.

(44) Stogryn, D. E.; Stogryn, A. P. *Mol. Phys.* **1966**, *11*, 371.

(45) Copeland, R. A.; Dyer, M. J.; Crosley, D. R. *J. Chem. Phys.* **1985**, *82*, 4022.